

## Multiple micro-cavity vibro-polaritons formation with different vibrational bands of the methylene group

Mario Malerba<sup>1</sup>, Mathieu Jeannin, Paul Goulain, Adel Bousseksou, Raffaele Colombelli, Jean-Michel Manceau\*

Centre de Nanosciences et Nanotechnologies, Université Paris-Saclay, CNRS, UMR 9001, Palaiseau 91120, France

### ARTICLE INFO

#### Keywords:

Vibro-polaritons  
Organic material  
Thin film  
Spectroscopy

### ABSTRACT

We present an experimental technique to accurately predict the formation of vibro-polaritons from a molecular polymeric film embedded in a resonant mid-infrared cavity. Using simple Fourier-transform reflectance measurement, we extract the complex dielectric function of a polyethylene film using Kramers-Kronig relations. The fitted dielectric function can be plugged into a numerical code to predict the strength and dispersion of the strong light-matter coupling regime between the quantized electromagnetic modes of a microcavity and the vibrational bands of the molecules. As a demonstration, we experimentally resolve the simultaneous formation of multiple vibro-polariton modes issued from the strong coupling of some vibrational bands of the methylene group ( $\text{CH}_2$ ) in a 2.5- $\mu\text{m}$ -thick polyethylene film embedded in a microcavity. We measure a Rabi splitting of 6.3 THz for the stretching doublet around 87.5 THz and a Rabi splitting of 1.1 THz for the scissoring doublet around 43.7 THz, in excellent agreement with numerical predictions.

Engineering of the light-matter interaction has been one of the most blossoming field of modern physics over the past two decades. In particular, when the losses of a two-level system and a resonant microcavity modes are lower than their coupling constant, one can observe a lift of degeneracy between the two modes, with an anti-crossing behavior of the new eigenstates separated by twice the vacuum Rabi frequency. These hybrid light-matter states, usually named polaritons, have been demonstrated in a plethora of systems. In particular in the near-infrared range exciton-polaritons in inorganic and organic materials have led to spectacular effects like room temperature Bose-Einstein condensation and conductivity enhancement [1–4]. At mid ( $\lambda=3\text{--}30\ \mu\text{m}$ ) and far ( $\lambda=30\text{--}100\ \mu\text{m}$ ) infrared wavelengths, inter-subband polaritons have been the work-horse for the exploration of bosonicity [5,6] and the first demonstrations of the ultrastrong coupling regime [7,8]. More than the strict fundamental aspect, they have been shown as a promising approach for the development of optoelectronic components such as modulators and saturable absorber [9–13].

In recent years, novel polaritonic system have emerged in this frequency range (3–100  $\mu\text{m}$ ). Using organic materials, the vibrational bands of molecules have been placed at the vicinity of resonant micro-cavities to enter the so-called vibrational strong-coupling (VSC) regime

[14–16]. Such interaction has already been demonstrated with various solid-phase molecular systems, but also under liquid phase within a microfluidic cavity [17]. This regime offers important perspectives from a chemistry point of view [18,19], with for instance the demonstration of the control over a reaction selectivity without illumination [20]. Ultrafast pump-probe spectroscopy, that aims at exploring the intermolecular vibrational energy transfer and relaxation within these dressed vibrational states, has also been explored [21,22]. Along with the possibilities brought on the control of molecular properties, these systems also appear as potential candidates for photonic devices, with the exploration of parametric processes under resonant optical pumping scheme. The perspective is to demonstrate final state stimulation [6] or different types of optical parametric oscillators where the Raman active mode is dressed with a secondary micro-cavity mode, as proposed for instance in [23].

In this respect, gaining a precise control over the design and the fabrication of the cavity, as well as the planarity of the molecular film placed within the cavity, is of great importance. So far, little effort has been devoted to the optimization, design and precise measurement of the strongly coupled system. Few attempts to improve the lifetime of the photonic system using Bragg mirrors have been reported [24,25] along

\* Corresponding author.

E-mail address: [jean-michel.manceau@c2n.upsaclay.fr](mailto:jean-michel.manceau@c2n.upsaclay.fr) (J.-M. Manceau).

<sup>1</sup> Present address: INRIM Istituto Nazionale di Ricerca Metrologica, I- 10135 Turin, Italy

with approaches where the resonant EM mode is highly confined using nano-resonators supporting localized surface plasmon or phonon-polariton resonances [26–29]. More recently, placing molecules at the vicinity of a strongly localized electro-magnetic (EM) mode was also proposed as a platform for frequency up-conversion down to the single photon level [30], and was later demonstrated with mid-infrared (MIR) photons using molecules in conjunction with plasmonic resonators [31,32]. In both cases, the authors take advantage of the small mode volume and the Raman activity of molecules to upconvert MIR photons to the visible range.

In the present article, we report on a simple method to measure the complex dielectric function of a polyethylene thin film using a single port reflection geometry. From the spectroscopic measurement of the absorption, we use Kramers-Kronig relation to extract the real and imaginary part of the material permittivity. Using a numerical simulation code, we then show that we can accurately predict the behavior of the randomly organized molecular film when embedded in the micro-cavity. In particular, we predict the multiple vibro-polariton formations and the system's inherent coupling Rabi frequency, using an analytical expression that links quantum formulation and classical calculation. To illustrate our approach, we experimentally resolved the polaritonic dispersion formed once a film of polyethylene is covered by a semi-transparent mirror, hence forming a Fabry-Perot cavity. Remarkably, we show that the strong light-matter coupling occurs simultaneously at the scissoring and stretching bands of the methylene group ( $\text{CH}_2$ ). Numerical predictions are in excellent agreement with the experimental demonstration. Our single port experiment appears as a valuable tool for the precise design and characterization of optically pumped vibro-polaritonic systems and particularly relevant for the exploration of different molecular film structural organizations. Although the present demonstration is done with Fabry-Perot microcavity, it could be extended to other plasmonic or sub-wavelength systems.

As active vibrational material, we have chosen one of the most common commercial thermoplastics, namely the mid-density

polyethylene (MDPE, Sigma-Aldrich), a polymer made of long hydrocarbon chains of ethylene monomer ( $\text{C}_2\text{H}_4$ ). Polyethylene has a long history as a Raman active material and presents sharp vibrational bands at MIR wavelengths [33–36], which makes it compatible with the theoretical proposal in [23] to make a parametric oscillator. More recently, we have used such film as thermal transducer for near-field measurement of the strong light matter coupling in a single nano-resonator [37]. In this paper, we use polyethylene as a thermal transducer to locally probe the confined EM mode. In the present work, the molecular film is obtained from a classic spin coating approach. Molecules under solid form are dissolved in decahydronaphthalene, a solvent than can be heated up to  $190\text{ }^\circ\text{C}$ . The melting temperature of polyethylene occurs at around  $140\text{ }^\circ\text{C}$ . The solution is spin-coated on a glass substrate previously metallized with a  $200\text{ nm}$  thick gold film, which constitutes the bottom mirror of the Fabry-Perot (FP) cavity. Hence, we are in presence of a system presenting a single optical access port as depicted in Fig. 1a: this allows us to characterize the material and retrieve the basic optical parameters with a single reflectivity measurement, as explained in the next paragraphs. The glass substrate is kept at high temperature during the coating process to avoid precipitation of condensed solid flakes of MDPE during the spinning and maintain the desired viscosity ensuring reproducibility in the film thickness. After spin-coating, the sample is annealed at  $150\text{ }^\circ\text{C}$  in order to fully evaporate all the solvent and is then abruptly tempered into cold water in order to keep the amorphous character within the film organization. Using a reflectometer, we determined a film thickness around  $1.3\text{ }\mu\text{m}$ .

First, we spectrally characterized the bare film sample using a Fourier transform infrared spectrometer equipped with a reflection angle motorized unit that allows the precise positioning of impinging light angle (Fig. 1a). We used a SiC (Silicon Carbide) globar source in conjunction with a KBr (Potassium Bromide) beam splitter and a room temperature DTGS (Deuterated Triglycine sulfate) detector. We can control the polarization of the impinging light using a KRS-5 (Thallium

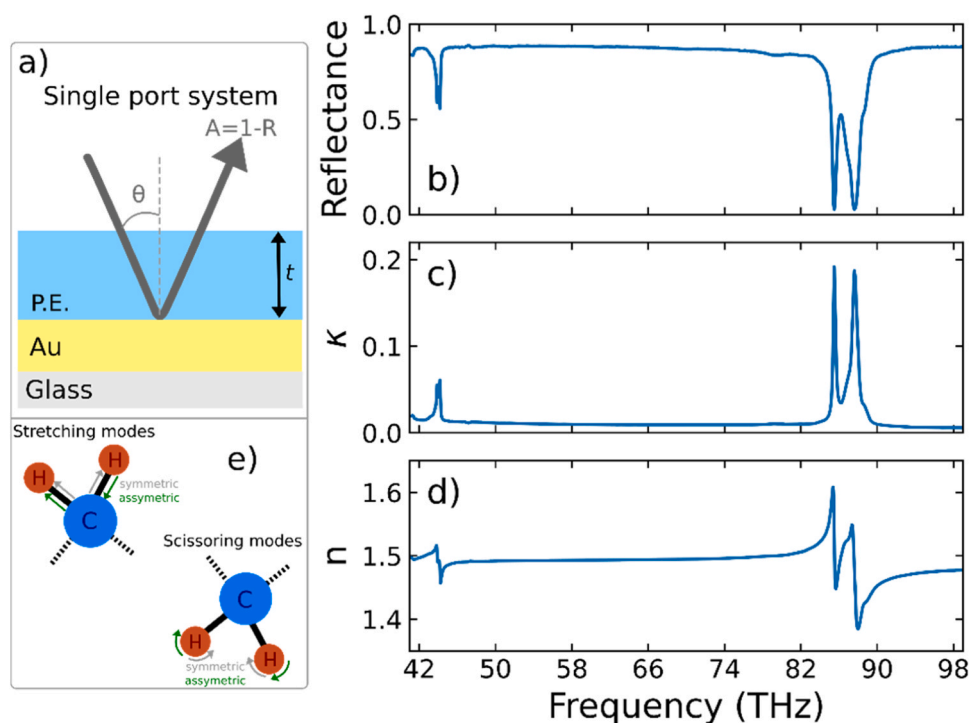


**Fig. 1.** Schematic representation of the experimental single port approach. The ground mirror is thick enough ( $200\text{ nm}$ ) so the system can only be probed in reflection using a motorized angle unit inserted within an FTIR spectrometer. (b) Reflectance measurement of the bare ( $1.3\text{ }\mu\text{m}$  thick) polyethylene film. (c) Extracted imaginary part of the refractive index. (d) Real part of the refractive index calculated using Kramers-Kronig relation. (e) Schematic representation of the in-plane stretching and scissoring modes of the ethylene monomer.

Halogenide) polarizer. The bare MDPE film is probed at an incidence angle of 13 degrees. As presented in Fig. 1b, the methylene group (CH<sub>2</sub>), constituting the MDPE polymeric film, exhibits two distinctive absorption bands that are evenly spaced in frequency, the scissoring modes at ~43.7 THz and the stretching modes at ~87.5 THz, as already assigned in a vast body of literature [33–36]. They are doublets oscillating at a symmetric and anti-symmetric resonance as schematically represented in Fig. 1e. Our single-port experimental geometry enables an accurate estimation of the dielectric function of the bare PE film ( $n$ ,  $k$ ). In fact, from the absorbance measurement on the bare film on gold (Au) (Fig. 1b), one can use Beer-Lambert's law to deduce the imaginary part of the refractive index (Fig. 1c). It is important to note that this approach suffers limitations as sample thicknesses in the range of  $\lambda/2n$  and  $\lambda/4n$  (and any multiple of these thicknesses) must be avoided. In such configuration constructive and destructive interferences could severely change the intensity of the measured vibrational bands. Using the Kramers-Kronig relation, the real part of the refractive index function can be calculated over our frequency range of interest as shown in Fig. 1d and described in [38,39]. Note that, field enhancement effects occurring at the mirror interface or within microcavity have not been considered when calculating the polaritons formation, since the field intensity has no effect on the vacuum Rabi splitting. Hence the complex permittivity function can be retrieved. We then fit these data with a multiple Lorentz permittivity model using the following expression:

$$\epsilon(\omega) = \epsilon_b - \sum_{k=1}^n \frac{2a_k\omega_k}{\omega^2 - \omega_k^2 + i\omega\gamma_k} \quad (1)$$

We use the formalism developed in [40], where  $a_k$ ,  $\omega_k$  and  $\gamma_k$  are the amplitude, the frequency and the decay rate of each resonance. The background permittivity,  $\epsilon_b$ , is equal to 2.2. Fig. 2a,b,c,d show the good agreement in between the extracted permittivity and the Lorentz model for both vibrational set of doublets. Nevertheless, we note a slight discrepancy on the background of the imaginary part that is not captured by our fit. We attribute it to a combination of Fresnel reflection

at the interfaces and Mie scattering within the amorphous film that leads a background absorption away from the vibrational modes of interest. This background absorption is small enough to be considered negligible in [41], where polyethylene is used to probe strong light matter coupling at the single resonator level. We provide the fitting values within the Table S1.

This fitted permittivity can then be plugged into numerical simulations to predict the organic polaritonic system dispersion with high accuracy. In particular, it allows to precisely design the film thickness in order to get simultaneously the different vibrational bands coupled to the 1st and 2nd Fabry-Perot modes of the micro-cavity. Fig. 2e shows the numerical simulations obtained from a rigorous coupled wave analysis code (RCWA) [42,43], where we have used a molecular film of 2.6  $\mu\text{m}$ . The gold permittivity is taken from [44] and the semi-transparent top mirror is 20 nm thick. From this simulation, one can clearly observe the lift of degeneracy for both vibrational bands and the apparition of the new hybridized polaritonic states. In fact, we can also use the extracted permittivity parameters with the formalism developed in [40] in order to estimate the minimum Rabi splitting frequency of such system when placed at the vicinity of a microcavity. This formalism links quantum formulation and classical calculation, providing a simple analytical expression that allows us to estimate the minimum Rabi splitting:

$$\Omega_S = \sum_{k=1}^n \sqrt{\frac{a_k\omega_k}{\epsilon_b} f_w} = 2\Omega_R \quad (2)$$

where  $f_w$  is an overlap factor between the confined EM mode and the active molecular film. In the present case of a FP cavity, this value is equal to 1. Starting with the stretching modes, the above calculation gives a Rabi splitting value of 6.4 THz between the lower and upper polaritonic states and 1.4 THz for the scissoring modes.

To validate the predictivity of our approach, we thus realized experimentally the previously described sample. We spin-coat a molecular film of 2.56  $\mu\text{m}$  thickness (measured using a reflectometer) on which we deposited 20 nm of gold, as depicted in the inset of Fig. 3a. We

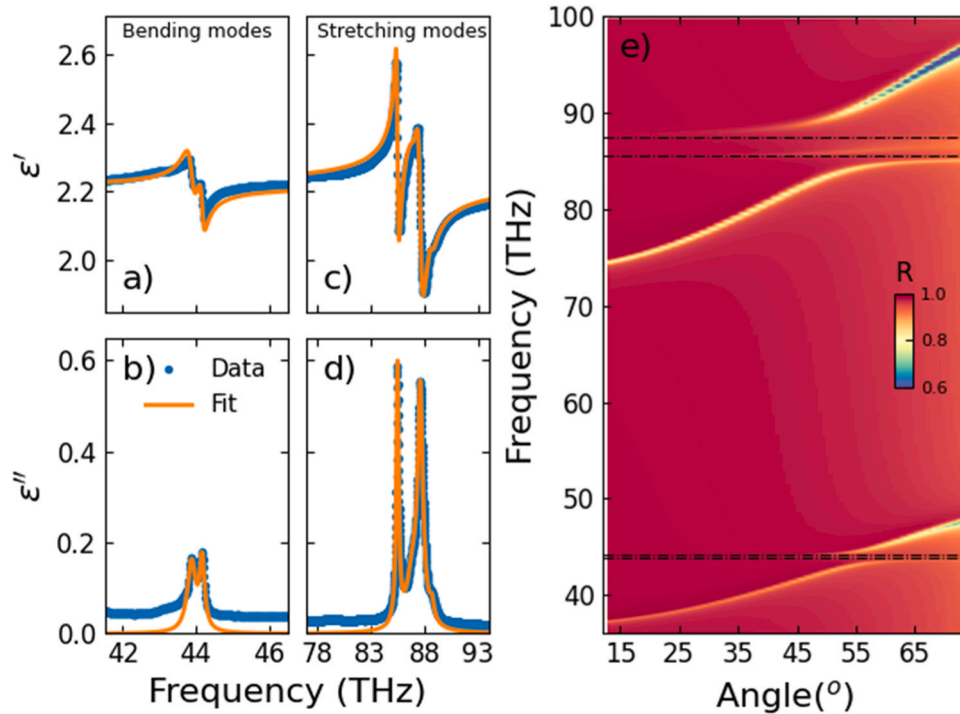


**Fig. 2.** (a,b,c,d) Fitting curves of the extracted dielectric function from the PE film using a multiple Lorentz oscillator permittivity model for both scissoring and stretching modes. On the upper panels are the real parts, while the lower ones show the imaginary parts (e) RCWA numerical simulation of the reflectance from a 2.6  $\mu\text{m}$  polyethylene film embedded in a single port microcavity. The fitted permittivity is used to depict the polyethylene film. One clearly sees the lift of degeneracy for both vibrational bands and the simultaneous formation of polariton modes with the 1st and 2nd mode of the Fabry-Perot microcavity.

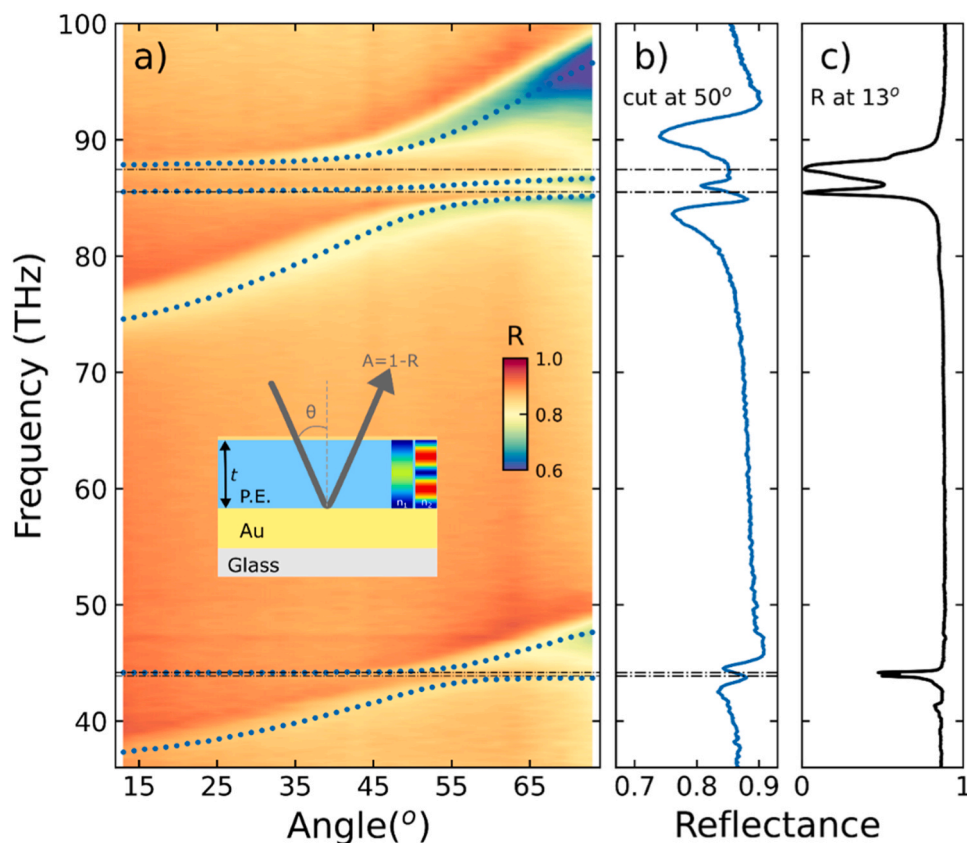


**Fig. 3.** (a) Experimental angle-resolved reflectance of the 2.56  $\mu\text{m}$  PE film embedded in the double metal FP micro-cavity. Both scissoring and stretching vibrational modes are coupled to the  $n_1$  and  $n_2$  FP cavity modes. We can resolve the polaritonic branches dispersion. The blue dots correspond to the reflectance minima extracted from the simulation of Fig. 2e. The black dash line indicates the position of the vibrational bands. In inset, schematic of the microcavity in the strong coupling regime with the PE probed in reflectance with a FTIR spectrometer. The electric field distribution of both resonant EM modes is also shown. (b) Reflectance cut at the anti-crossing ( $50^\circ$ ) of the PE film embedded in FP microcavity. (c) Reflectance of the bare PE film spin-coated on the gold surface taken at an angle of 13 degrees. Both scissoring and stretching doublets of the ethylene monomer ( $\text{CH}_2$ ) can be resolved with an experimental resolution of  $2\text{ cm}^{-1}$ .

then probed the reflectivity  $R(\omega, \theta)$  of the formed microcavity over a large spectral bandwidth (18–210 THz) and a wide angular range ( $13^\circ < \theta < 73^\circ$ ). The impinging radiation is TM (Transverse Magnetic) polarized, ensuring a stronger contrast of the photonic mode. The absolute reflectivity is obtained by division of the sample spectrum with a reference one taken from a planar gold surface as shown in [45]. The experimental dispersion of the polaritonic modes is presented in Fig. 3a. The eigenstates originating from the strong coupling regime are clearly resolved and exhibit the characteristic anti-crossing signature of the polaritonic modes. The scissoring and the stretching band doublets are coupled to the 1st and 2nd Fabry-Perot modes, showing a simultaneous coupling of different vibrational bands within the ethylene monomer. While three distinct polaritonic branches are observed in the case of the stretching band, we were able to resolve only two branches in the case of the scissoring mode even with an increased resolution of 60 GHz, due to the very weak contrast of the central branch. We have experimentally measured a Rabi splitting of 6.35 THz for the stretching doublet and 1.14 THz for the scissoring one, in good agreement with the previously calculated values. The simulated reflectivity minima are superimposed (blue dots) on the reflectance color-plot and their spectral positions match very well with the numerical simulation. Fig. 3b,c show reflectance cuts of the micro-cavity sample at the anti-crossing angle ( $50^\circ$ ) and the bare film at  $13^\circ$  incidence.

The linewidth of the calculated polaritonic branches is significantly smaller if compared to the experiment, while the trend of the resonant mode contrast is similar. Two factors could explain this difference: (i) the angular broadening from the measurement system in contrast with the plane-wave used in numerical simulation and (ii) local spatial

variations in PE film thickness, which can introduce a strong broadening. To this regard, we checked the film thickness at different locations by probing the sample's local optical response with a microscope FTIR (Fig. 4), equipped with a Cassegrain 15X objective and using a 150  $\mu\text{m}$  sided square spot area. Using the analytical expression of a FP resonant mode  $\nu_k = kc/2nL$ , where  $L$  is the thickness of the film and  $n$  the refractive index, we have estimated using the 3rd order FP mode, a disparity of about 160 nm in thickness over a  $1\text{ mm}^2$  sample area. This observation contrasts with AFM (atomic force microscope) measurements of the local roughness that have shown a film roughness of about 10 nm over tens of microns length. Such long-range modulation of the film thickness is the direct result of the spin-coating technique that can generate ripples if solvent evaporation is not thoroughly optimized. In turn, gaining a higher degree of control over the film thickness would be beneficial for photonic applications where the dressed state lifetime is involved and techniques such as dip coating could be employed [46]. This further confirms that the single port experimental approach we have presented is a powerful tool in view of designing and optimizing molecular films. With accurate control over the bare molecular film thickness, one can precisely predict the expected Rabi splitting frequency – and the full dispersion – once the film is placed in the micro-cavity. Therefore, any attempt to optimize the polymeric orientation to obtain – for instance – a crystal like orientation with a higher number of aligned dipoles could be gauged rapidly and precisely with a simple reflectance measurement [33,34]

In conclusion, we have shown a simple approach based on reflectance measurements of a single port system to accurately extract the complex dielectric function of a bare molecular film. It can be fitted with

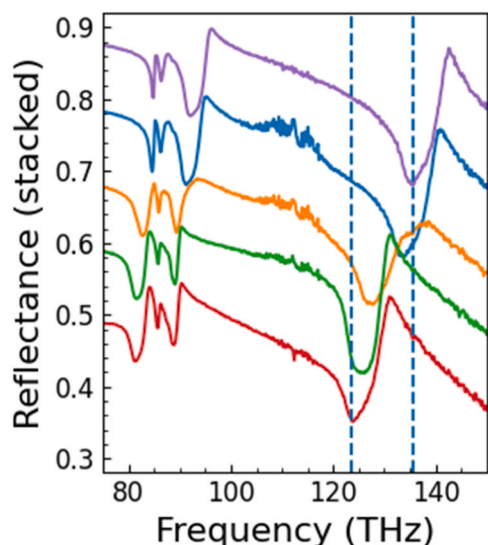


**Fig. 4.** Reflectance of the strongly-coupled sample probed using a FTIR microscope with a 150  $\mu\text{m}$  square focal spot. Probing at different position over a 1 mm distance shows a 3rd FP mode resonant at different frequencies, which indicates a thickness disparity of about 160 nm.

a simple Lorentz oscillator permittivity model and plugged into numerical simulations to accurately predict polaritons dispersion and analytically estimate the light-matter coupling strength. We experimentally validated this approach with the detection of multiple polaritons, formed from different vibrational modes of the same ethylene monomer placed in a resonant Fabry-Perot microcavity. The formation of polaritonic modes involving different photonic and vibrational modes could be a useful resource for non-linear experiments exploiting e.g. vibrational intermode coupling or multiply-resonant features.

#### CRediT authorship contribution statement

**Adel Bousseksou:** Investigation, Formal analysis. **Paul Goulain:** Investigation, Formal analysis. **Mathieu Jeannin:** Writing – original draft, Investigation, Formal analysis. **Mario Malerba:** Writing – original draft, Investigation, Conceptualization. **Jean-Michel Manceau:** Writing – review & editing, Writing – original draft, Supervision, Funding acquisition, Formal analysis, Conceptualization. **Raffaele Colombelli:** Writing – original draft, Funding acquisition, Formal analysis.

#### Declaration of Competing Interest

The authors declare that they have no known competing financial interests or personal relationships that could have appeared to influence the work reported in this paper.

#### Data availability

Data will be made available on request.

#### Acknowledgments

We warmly thank M. Manceau, A. Cattoni and J. Feist for useful discussions while initiating this research activity. We acknowledge financial support from the European Union FET-Open Grant MIRBOSE (737017) and from the French National Research Agency (Projects ANR-19-CE24-0003 “SOLID” and ANR-17-CE24-0016 “IRENA”). M.M. acknowledges financial support from the Marie Skłodowska Curie Action, Grant Agreement No. 748071. This work was partially supported by the French RENATECH network.

#### Appendix A. Supporting information

Supplementary data associated with this article can be found in the online version at doi:10.1016/j.photonics.2024.101294.

#### References

- [1] J. Kasprzak, M. Richard, S. Kundermann, A. Baas, P. Jeambrun, J.M.J. Keeling, F. M. Marchetti, M.H. Szymańska, R. André, J.L. Staehli, V. Savona, P.B. Littlewood, B. Deveaud, L.S. Dang, Bose-Einstein condensation of exciton polaritons, *Nature* 443 (7110) (2006) 409–414.
- [2] S. Kéna-Cohen, S.R. Forrest, Room-temperature polariton lasing in an organic single-crystal microcavity, *Nat. Photon* 4 (6) (2010) 371–375.
- [3] E. Orgiu, J. George, J.A. Hutchison, E. Devaux, J.F. Dayen, B. Doudin, F. Stellacci, C. Genet, J. Schachenmayer, C. Genes, G. Pupillo, P. Samori, T.W. Ebbesen, Conductivity in organic semiconductors hybridized with the vacuum field, *Nat. Mater.* 14 (11) (2015) 1123–1129.
- [4] D. Sanvitto, S. Kéna-Cohen, The road towards polaritonic devices, *Nat. Mater.* 15 (10) (2016) 1061–1073.
- [5] S. De Liberato, C. Ciuti, Stimulated Scattering and Lasing of Intersubband Cavity Polaritons, *Phys. Rev. Lett.* 102 (13) (2009) 136403.
- [6] M. Knorr, J.M. Manceau, J. Mornhinweg, J. Nespolo, G. Biasiol, N.-L. Tran, M. Malerba, P. Goulain, X. Lafosse, M. Jeannin, M. Stefinger, I. Carusotto, C. Lange, R. Colombelli, R. Huber, Intersubband Polariton-Polariton Scattering in a Dispersive Microcavity, *Phys. Rev. Lett.* 128 (24) (2022) 247401.
- [7] A.A. Anappara, S. De Liberato, A. Tredicucci, C. Ciuti, G. Biasiol, L. Sorba, F. Beltram, Signatures of the ultrastrong light-matter coupling regime, *Phys. Rev. B* 79 (20) (2009) 201303.
- [8] Y. Todorov, A.M. Andrews, R. Colombelli, S. De Liberato, C. Ciuti, P. Klang, G. Strasser, C. Sirtori, Ultrastrong Light-Matter Coupling Regime with Polariton Dots, *Phys. Rev. Lett.* 105 (19) (2010) 196402.
- [9] A.A. Anappara, A. Tredicucci, F. Beltram, G. Biasiol, L. Sorba, Tunnel-assisted manipulation of intersubband polaritons in asymmetric coupled quantum wells, *Appl. Phys. Lett.* 89 (17) (2006) 171109.
- [10] J. Lee, S. Jung, P.-Y. Chen, F. Lu, F. Demmerle, G. Boehm, M.-C. Amann, A. Alù, M. A. Belkin, Ultrafast Electrically Tunable Polaritonic Metasurfaces, *Adv. Opt. Mater.* 2 (11) (2014) 1057–1063.
- [11] S. Pirotta, N.-L. Tran, A. Jollivet, G. Biasiol, P. Crozat, J.-M. Manceau, A. Bousseksou, R. Colombelli, Fast amplitude modulation up to 1.5 GHz of mid-IR free-space beams at room-temperature, *Nat. Commun.* 12 (1) (2021) 799.
- [12] M. Jeannin, J.-M. Manceau, R. Colombelli, Unified description of saturation and bistability of intersubband transitions in the weak and strong light-matter coupling regimes, *Phys. Rev. Lett.* 127 (18) (2021) 187401.
- [13] M. Jeannin, E. Cosentino, S. Pirotta, M. Malerba, G. Biasiol, J.-M. Manceau, R. Colombelli, Low intensity saturation of an ISB transition by a mid-IR quantum cascade laser, *Appl. Phys. Lett.* 122 (24) (2023) 241107.
- [14] A. Shalabney, J. George, J. Hutchison, G. Pupillo, C. Genet, T.W. Ebbesen, Coherent coupling of molecular resonators with a microcavity mode, *Nat. Commun.* 6 (1) (2015) 5981.
- [15] B.S. Simpkins, K.P. Fears, W.J. Dressick, B.T. Spann, A.D. Dunkelberger, J. C. Owrutsky, Spanning Strong to Weak Normal Mode Coupling between Vibrational and Fabry-Pérot Cavity Modes through Tuning of Vibrational Absorption Strength, *ACS Photonics* 2 (10) (2015) 1460–1467.
- [16] R. Damari, O. Weinberg, D. Krotkov, N. Demina, K. Akulov, A. Golombek, T. Schwartz, S. Fleischer, Strong coupling of collective intermolecular vibrations in organic materials at terahertz frequencies, *Nat. Commun.* 10 (1) (2019) 3248.
- [17] J. George, A. Shalabney, J.A. Hutchison, C. Genet, T.W. Ebbesen, Liquid-Phase Vibrational Strong Coupling, *J. Phys. Chem. Lett.* 6 (6) (2015) 1027–1031.
- [18] M. Hertzog, M. Wang, J. Mony, K. Börjesson, Strong light-matter interactions: a new direction within chemistry, *Chem. Soc. Rev.* 48 (3) (2019) 937–961.
- [19] K. Hirai, J.A. Hutchison, H. Uji-i, Recent Progress in Vibropolaritonic Chemistry, *ChemPlusChem* 85 (9) (2020) 1981–1988.
- [20] A. Thomas, L. Lethuillier-Karl, K. Nagarajan, R.M.A. Vergauwe, J. George, T. Chervy, A. Shalabney, E. Devaux, C. Genet, J. Moran, T.W. Ebbesen, Tilting a ground-state reactivity landscape by vibrational strong coupling, *Science* 363 (6427) (2019) 615–619.
- [21] B. Xiang, R.F. Ribeiro, M. Du, L. Chen, Z. Yang, J. Wang, J. Yuen-Zhou, W. Xiong, Intermolecular vibrational energy transfer enabled by microcavity strong light-matter coupling, *Science* 368 (6491) (2020) 665–667.
- [22] A.D. Dunkelberger, B.T. Spann, K.P. Fears, B.S. Simpkins, J.C. Owrutsky, Modified relaxation dynamics and coherent energy exchange in coupled vibration-cavity polaritons, *Nat. Commun.* 7 (1) (2016) 13504.
- [23] J. del Pino, F.J. Garcia-Vidal, J. Feist, Exploiting Vibrational Strong Coupling to Make an Optical Parametric Oscillator Out of a Raman Laser, *Phys. Rev. Lett.* 117 (27) (2016) 277401.
- [24] M. Muallem, A. Palatnik, G.D. Nessim, Y.R. Tischler, Strong Light-Matter Coupling and Hybridization of Molecular Vibrations in a Low-Loss Infrared Microcavity, *J. Phys. Chem. Lett.* 7 (11) (2016) 2002–2008.
- [25] O. Kapon, R. Yitzhary, A. Palatnik, Y.R. Tischler, Vibrational Strong Light-Matter Coupling Using a Wavelength-Tunable Mid-infrared Open Microcavity, *J. Phys. Chem. C* 121 (34) (2017) 18845–18853.
- [26] H. Memmi, O. Benson, S. Sadofev, S. Kalusniak, Strong Coupling between Surface Plasmon Polaritons and Molecular Vibrations, *Phys. Rev. Lett.* 118 (12) (2017) 126802.

- [27] M. Autore, P. Li, I. Dolado, F.J. Alfaro-Mozaz, R. Esteban, A. Atxabal, F. Casanova, L.E. Hueso, P. Alonso-González, J. Aizpurua, A.Y. Nikitin, S. Vélez, R. Hillenbrand, Boron nitride nanoresonators for phonon-enhanced molecular vibrational spectroscopy at the strong coupling limit, *Light Sci. Appl.* 7 (4) (2018).
- [28] T.G. Folland, G. Lu, A. Bruncz, J.R. Nolen, M. Tadjer, J.D. Caldwell, Vibrational Coupling to Epsilon-Near-Zero Waveguide Modes, *ACS Photonics* 7 (3) (2020) 614–621.
- [29] M. Hertzog, B. Munkhbat, D. Baranov, T. Shegai, K. Börjesson, Enhancing Vibrational Light–Matter Coupling Strength beyond the Molecular Concentration Limit Using Plasmonic Arrays, *Nano Lett.* (2021).
- [30] P. Roelli, D. Martin-Cano, T.J. Kippenberg, C. Galland, Molecular Platform for Frequency Upconversion at the Single-Photon Level, *Phys. Rev. X* 10 (3) (2020) 031057.
- [31] A. Xomalis, X. Zheng, R. Chikkaraddy, Z. Koczor-Benda, E. Miele, E. Rosta, G.A. E. Vandenbosch, A. Martínez, J.J. Baumberg, Detecting mid-infrared light by molecular frequency upconversion in dual-wavelength nanoantennas, *Science* 374 (6572) (2021) 1268–1271.
- [32] W. Chen, P. Roelli, H. Hu, S. Verlekar, S.P. Amirtharaj, A.I. Barreda, T. J. Kippenberg, M. Kovylyna, E. Verhagen, A. Martínez, C. Galland, Continuous-wave frequency upconversion with a molecular optomechanical nanocavity, *Science* 374 (6572) (2021) 1264–1267.
- [33] F.J. Boerio, Raman scattering in crystalline polyethylene, *J. Chem. Phys.* 52 (7) (1970) 3425.
- [34] M. Pigeon, R.E. Prud'homme, M. Pezolet, Characterization of molecular orientation in polyethylene by Raman spectroscopy, *Macromolecules* 24 (20) (1991) 5687–5694.
- [35] J.V. Gulmine, P.R. Janissek, H.M. Heise, L. Akcelrud, Polyethylene characterization by FTIR, *Polym. Test.* 21 (5) (2002) 557–563.
- [36] M.R. Jung, F.D. Horgen, S.V. Orski, V. Rodriguez C, K.L. Beers, G.H. Balazs, T. T. Jones, T.M. Work, K.C. Brignac, S.-J. Royer, K.D. Hyrenbach, B.A. Jensen, J. M. Lynch, Validation of ATR FT-IR to identify polymers of plastic marine debris, including those ingested by marine organisms, *Mar. Pollut. Bull.* 127 (2018) 704–716.
- [37] M. Malerba, S. Sotgiu, A. Schirato, L. Baldassarre, R. Gillibert, V. Giliberti, M. Jeannin, J.-M. Manceau, L. Li, A.G. Davies, E.H. Linfield, A. Alabastri, M. Ortolani, R. Colombelli, Detection of Strong Light–Matter Interaction in a Single Nanocavity with a Thermal Transducer, *ACS Nano* 16 (12) (2022) 20141–20150.
- [38] W.R.M. Rocha, S. Pilling, Determination of optical constants  $n$  and  $k$  of thin films from absorbance data using Kramers–Kronig relationship, *Spectrochim. Acta Part A: Mol. Biomol. Spectrosc.* 123 (2014) 436–446.
- [39] V. Lucarini, J.J. Saarinen, K.-E. Peiponen, E.M. Vartiainen, *Kramers-Kronig Relations in Optical Materials Research*, Springer-Verlag, Berlin Heidelberg, 2005.
- [40] D.R. Abujetas, J. Feist, F.J. García-Vidal, J.G. Rivas, J.A. Sánchez-Gil, Strong coupling between weakly guided semiconductor nanowire modes and an organic dye, *Phys. Rev. B* 99 (20) (2019) 205409.
- [41] M. Malerba, S. Sotgiu, A. Schirato, L. Baldassarre, R. Gillibert, V. Giliberti, M. Jeannin, J.-M. Manceau, L. Li, A.G. Davies, E.H. Linfield, A. Alabastri, M. Ortolani, R. Colombelli, Detection of Strong Light–Matter Interaction in a Single Nanocavity with a Thermal Transducer, *ACS Nano* (2022).
- [42] S. Zanotto, “PPML - Periodically Patterned Multi Layer,” (2021).
- [43] J.-M. Manceau, S. Zanotto, I. Sagnes, G. Beaudoin, R. Colombelli, Optical critical coupling into highly confining metal-insulator-metal resonators, *Appl. Phys. Lett.* 103 (9) (2013) 091110.
- [44] R.L. Olmon, B. Slovick, T.W. Johnson, D. Shelton, S.-H. Oh, G.D. Boreman, M. B. Raschke, Optical dielectric function of gold, *Phys. Rev. B* 86 (23) (2012) 235147.
- [45] J.-M. Manceau, S. Zanotto, T. Ongarello, L. Sorba, A. Tredicucci, G. Biasiol, R. Colombelli, Mid-infrared intersubband polaritons in dispersive metal-insulator-metal resonators, *Appl. Phys. Lett.* 105 (8) (2014) 081105.
- [46] P. Yimsiri, M.R. Mackley, Spin and dip coating of light-emitting polymer solutions: Matching experiment with modelling, *Chem. Eng. Sci.* 61 (11) (2006) 3496–3505.